Journal of Materials Chemistry B

ROYAL SOCIETY OF CHEMISTRY

PAPER

View Article Online
View Journal | View Issue

Check for updates

Cite this: J. Mater. Chem. B, 2024, 12, 6840

A water-soluble luminescent tris(2,4,6-trichlorophenyl)methyl radical-carbazole dyad†

Kosuke Anraku,[a] Kenshiro Matsuda,[a] Satoshi Miyata,[bc] Hikaru Ishii,[c] Takuya Hosokai,*[bc] Satoshi Okada,[d] Kazuhiro Nakamura,[a] Kohei Nakao[e] and Ken Albrecht*[e]

Received 1st May 2024,
Accepted 6th June 2024

DOI: 10.1039/d4tb00940a

rsc.li/materials-b

Organic luminescent radicals are a new class of materials with potential applications not only in light-emitting devices but also in the biochemistry field. New tris(2,4,6-trichlorophenyl)methyl (**TTM**) radicals with alkoxy-substituted carbazole donors were synthesized and characterized. PEG-substituted carbazole-**TTM** was found to be water-soluble. The water-soluble **TTM** radical aqueous solution showed fluorescence at 777 nm and the ability to shorten the longitudinal relaxation time (T_1) of water. The concept of water-soluble luminescent radicals is expected to be used to develop a potential fluorescence and MR dual-use imaging moiety.

Introduction

Organic luminescent radicals are attractive for various applications, such as OLEDs, bioimaging, and sensing, due to their unique luminescence properties.[1–11] In general, radicals are unstable under an ambient atmosphere and are highly reactive species, and they are recognized as luminescent quenchers rather than luminophores. Recently, some stable organic radicals have been discovered as luminescent materials through ingenious molecular design strategies. Tris(2,4,6-trichlorophenyl)methyl (**TTM**) and perchlorotriphenylmethyl (PTM) radicals have been known as stable luminescent radicals, which are isolatable under atmospheric conditions.[12,13] The stability of chlorinated trityl radicals is ascribed largely to the steric protection of the center carbon with chlorine atoms at the *ortho* position and the delocalization of spin density over three π-conjugated systems. However, bare luminescent trityl radicals are known to have low photostability, and several strategies to improve photostability are proposed.[14,15] For example, attaching a donor molecule such as carbazole to have a charge transfer excited state character is the most widely accepted method.[16–19] Another approach is to add a heterocycle, such as pyridine, to decrease the energy of the frontier orbitals (PyBTM).[20] Halogenated trityl radicals are the most widely studied luminescent radicals, and a great effort has been made to improve the photoluminescence (PL) quantum yield (PLQY) and photostability.

Organic radicals have potential applications as magnetic resonance imaging (MRI) contrast agents due to their paramagnetic properties.[21–24] Typical MRI is an imaging technique that detects proton nuclei in water, fat, and other substances and produces contrast images based on differences in their relaxation times. The relaxation time of protons around a paramagnetic molecule is shortened by the weak local magnetic field generated by the molecule. Currently, Gd complexes are being used as clinical imaging contrast agents because they give MRI images with good contrast due to the highest spin quantum number (S = 7/2) of the Gd(III) ion.[22,25,26] However, side effects such as nephrogenic systemic fibrosis and accumulation of Gd in the brain are considered problematic. On the other hand, organic radicals have lower toxicity and are a promising candidate for electron spin resonance (ESR) or MR imaging even though they have smaller spin quantum numbers.[27] Several organic radicals based on 2,2,6,6-tetramethylpiperidine 1-oxyl (TEMPO) as ESR or MR imaging agents have been reported.[19–22]

TTM radical derivatives have attracted much attention due to their atmospheric stability, paramagneticity, and unique luminescence properties.[28] **TTM-Cz**, which has a carbazole donor and a **TTM** acceptor, has been extensively studied because of the photostability, high PLQY, and ease in modification of the carbazole moiety.[29–32] Due to the red to near-infrared (NIR) emission of **TTM-Cz** derivatives, they are potential candidates for fluorescence bioimaging.[3,5,6] **TTM-Cz** is hydrophobic, and the low water

[a] Interdisciplinary Graduate School of Engineering Sciences, Kyushu University, 6-1 Kasuga-Koen, Kasuga-Shi, Fukuoka 816-8580, Japan
[b] Department of Pure and Applied Chemistry, Faculty of Science and Technology, Tokyo University of Science, 2641 Yamazaki, Noda, Chiba 278-8510, Japan
[c] National Institute of Advanced Industrial Science and Technology (AIST), Tsukuba Central 5, 1-1-1 Higashi, Tsukuba, Ibaraki 305-8565, Japan. E-mail: t.hosokai@aist.go.jp
[d] Laboratory for Chemistry and Life Science, Institute of Innovative Research, 4259 Nagatsuta-cho, Midori-ku, Yokohama, Kanagawa 226-8501, Japan
[e] Institute for Materials Chemistry and Engineering, Kyushu University, 6-1 Kasuga-Koen, Kasuga-Shi, Fukuoka 816-8580, Japan. E-mail: albrecht@cm.kyushu-u.ac.jp

† Electronic supplementary information (ESI) available. See DOI: https://doi.org/10.1039/d4tb00940a

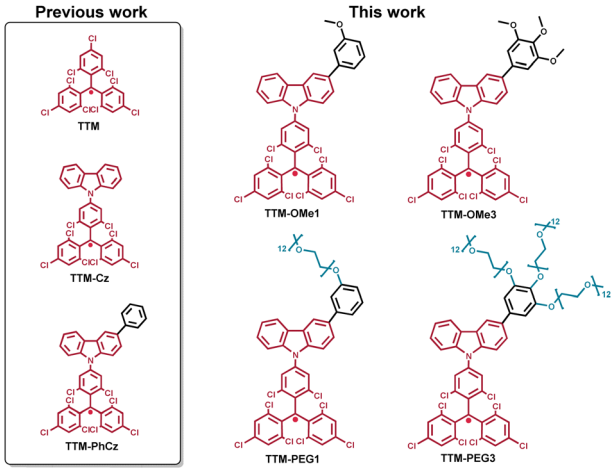

Fig. 1 Chemical structures of alkoxy-substituted **TTM** radical derivatives.

solubility limits its biological application. The currently reported strategy is to use surfactants and encapsulate radical nanoparticles to solubilize them in water.[3,5,6] The radical nanoparticles have potential for application in fluorescence imaging, but there is no report on their application as MR contrast agents and magnetic interaction with solvent water. Developing intrinsically water-soluble **TTM-Cz** derivatives will be a more straightforward approach to utilizing them for bioimaging applications. A few **TTM**s attached to the water-soluble or hydrophilic group have already been reported.[33–37] However, to our knowledge, a compound that shows water-solubility, luminescence, and paramagnetic relaxation enhancement (PRE) effects simultaneously has never been reported.

In this work, two methoxy substituted and two polyethyleneglycol substituted **TTM-Cz** radicals were designed and synthesized as water soluble luminescent radicals (Fig. 1). Their photophysical properties, solubility, and potential applications for fluorescence and MR imaging in water were investigated. The small and dual-functional imaging probe is assumed to be not harmful to biological activities. **TTM-PEG3** showed water solubility and NIR emission in an aqueous solution. Moreover, **TTM-PEG3** exhibited water-proton longitudinal relaxivity under aqueous conditions. This is the first water-soluble **TTM-Cz** radical derivative showing potential for fluorescence and MR dual imaging applications.

Results and discussion

Synthesis and characterization

New **TTM-Cz** radicals were synthesized *via* deprotonation and one-electron oxidation of precursors: HTTM-(OMe1, OMe3, PEG1, and PEG3) (Fig. S1, ESI†),[38–42] and radical precursors were synthesized by combining Suzuki–Miyaura cross-coupling and Williamson ether synthesis. The key compounds HTTM-OMe1 and HTTM-OMe3 were synthesized by Suzuki–Miyaura cross-coupling between boronated carbazole-HTTM (HTTM-BCz) and aryl halides.[32,34,35] The methoxy group was converted to a hydroxyl group with BBr_3 and reacted with tosylated polyethylene glycol (Ts-mPEG12) to obtain HTTM-PEG1 and HTTM-PEG3.[32,33,37] Obtained precursors were treated with KOtBu and then subsequently oxidized with *p*-chloranil to obtain the radicals. Precursors were characterized using ^{1}H NMR spectroscopy, ^{13}C NMR spectroscopy, MALDI-TOF-MS, and elemental analysis. Radicals were characterized using MALDI-TOF-MS, elemental analysis, and ESR spectroscopy. The purity of the radicals was determined by ESR spectroscopy to be around 79–98% by comparing the signal strength with that of the standard reference (TEMPOL). The impurities are considered to be the radical precursors because they cannot be separated due to their structural similarities. The impurities were confirmed to be the radical precursors by ^{1}H NMR. The new methoxylated and PEGylated **TTM** radical derivatives were successfully synthesized.

UV-vis absorption

The UV-vis absorption spectra of radicals were measured in toluene, chloroform, and water (Fig. 2a and Table 1). The new radicals in toluene showed identical spectral shapes with characteristic absorption bands at 377 nm attributed to the locally excited π–π^* transition of the **TTM** moiety. Absorption bands around 625 nm (**TTM-PhCz**: 622 nm,[28] **TTM-OMe1**: 623 nm, **TTM-OMe3**: 626 nm, **TTM-PEG1**: 624 nm, and **TTM-PEG3**: 629 nm) attributed to charge transfer (CT) from the carbazole donor to the **TTM** acceptor were also observed. For comparison,

UV-vis absorption and PL spectra of **TTM-PhCz** were also measured. Comparing **TTM-PhCz** (Fig. 1) and new radicals, the CT absorption band of new radicals was slightly red-shifted due to the electron-donating effect of the methoxy group. The molar

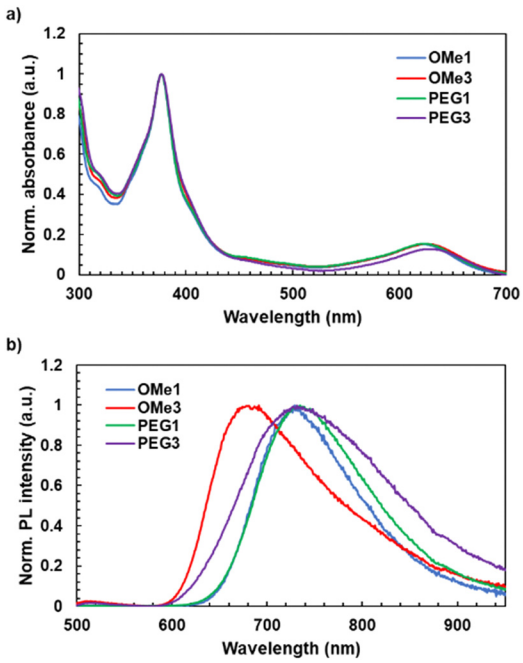

Fig. 2 (a) UV-vis absorption spectra of new methoxylated and PEGylated **TTM-Cz** radicals measured in toluene (10^{-5} M) and (b) PL spectra of new methoxylated and PEGylated **TTM-Cz** radicals measured at an absorbance of 1.0[–] at 377 nm (excitation wavelength) in toluene.

Table 1 Photophysical properties of alkoxy-substituted **TTM-Cz** radical derivatives

Compounds	λ_{abs}[a] (nm)	λ_{PL}[a] (nm)	PLQY[a] (%)	τ[b] (ns)	k_f[c] (10^6 s^{-1})	k_{nr}[d] (10^6 s^{-1})
TTM-PhCz	622[e]	722[e]	6.0[e]	5.0	12	190
TTM-OMe1	623	729	6.8	4.1	17	230
TTM-OMe3	626	691	0.3	31	0.10	33
TTM-PEG1	624	735	3.4	2.1	16	463
TTM-PEG3	623	731	0.2	4.2	0.48	239

[a] λ_{abs}: absorption, λ_{PL}: PL peak wavelength and PLQY: photoluminescence quantum yield measured in toluene solutions (10^{-5} M). [b] τ: PL lifetime measured at absorbance of 1.0[−] at 377 nm in toluene. [c] k_f: radiative decay rate. [d] k_{nr}: non-radiative decay rate. [e] These values were cited from ref. 28.

absorption coefficients (ε) were determined to be 4.8×10^3 M^{-1} cm^{-1}, 608 nm (**TTM-OMe1**), 4.6×10^3 M^{-1} cm^{-1}, 608 nm (**TTM-OMe3**), 4.6×10^3 M^{-1} cm^{-1}, 608 nm (**TTM-PEG1**), and 4.4×10^3 M^{-1} cm^{-1}, 610 nm (**TTM-PEG3**) in chloroform. Note that the ε values were corrected by the purity of radical compounds determined by ESR measurements, and the CT absorption peaks of new radicals in chloroform tend to appear at shorter wavelengths than those in toluene.[28,43] PEGylated **TTM**s were water soluble and showed almost the same absorption spectral shape as in toluene (Fig. 3). The absorbance of **TTM-PEG1** saturated aqueous solution prepared by filtration of the 10^{-4} M dispersion through a 0.20 μm pore size membrane filter was 0.047 (631 nm) which is about 1/10 times of **TTM-PEG3** after filtration (0.42, 634 nm). ε of **TTM-PEG3** in water was almost the same as that of **TTM-PEG3** in chloroform. This result suggests that the water-solubility limit of **TTM-PEG1** is smaller than 10^{-5} M, and that of **TTM-PEG3** is higher than 10^{-5} M (later, it will be shown to be higher than 10^{-2} M). The CT absorption peak of **TTM-PEG3** in water was located at 634 nm, and a slight bathochromic shift (5 nm) was observed compared to that in toluene. The aqueous solution of **TTM-PEG3** was transparent, and no light scattering was observed. Methoxy and PEG substitutions change the absorption and emission slightly, and **TTM-PEG3** is favorably water-soluble without any additives such as surfactants.

Dynamic light scattering (DLS) measurement of radicals was performed in toluene and water (1 mM) to understand the dissolved state of radicals in toluene and water (Fig. S14, ESI†). DLS measurements for **TTM-PEG3** with average hydrodynamic diameters in water showed broad and sharp bands distributed around 6 nm and 104 nm. On the other hand, all of the radicals showed no light scattering signal in toluene, indicating that they were in a single molecular state. The DLS results indicate that **TTM-PEG3** is water-soluble but tends to form aggregates in water.

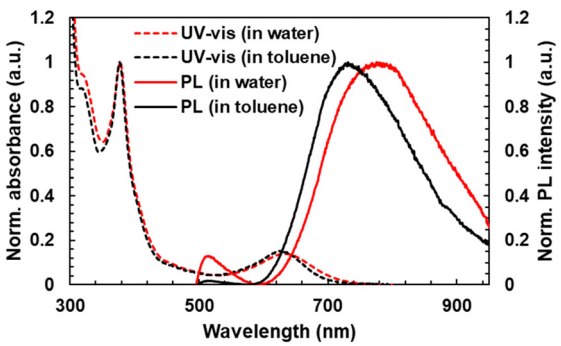

Fig. 3 (dotted line) UV-vis absorption and (real line) PL spectra of **TTM-PEG3** in (red) water (10^{-5} M) and (black) toluene (10^{-5} M) for comparison.

Photoluminescence properties

The PL spectra, PLQY, and PL lifetime (τ) in toluene and water were measured (Fig. 2b, Table 1). New radical compounds exhibited PL in the red to NIR region in toluene at 729 nm (OMe1), 691 nm (OMe3), 735 nm (PEG1), and 731 nm (PEG3), respectively. The PLQY was determined to be 6.8% (OMe1), 0.3% (OMe3), 3.4% (PEG1), and 0.2% (PEG3), respectively. When methoxylated radicals were compared to PEGylated radicals, the PLQY of PEGylated radicals was lowered. The non-radiative decay rates (k_{nr}) of **TTM-OMe1** (230×10^6 s^{-1}), **TTM-OMe3** (33×10^6 s^{-1}), **TTM-PEG1** (463×10^6 s^{-1}), **TTM-PEG3** (239×10^6 s^{-1}) in toluene were determined using τ and PLQY (Table 1, Fig. S18, ESI†). PEGylated radicals seem to have higher flexibility, resulting in lower PLQY caused by the higher k_{nr}. The PL spectra and PLQY of **TTM-PEG3** were also measured in water (Fig. 3). This water-soluble radicals exhibited detectable NIR emission with a low PLQY (777 nm, 0.006%) in water. Note that the PLQY value was determined by comparing the PL intensity of $[Ru(bpy)_3]Cl_2$ with the radical emission.[44] To understand in detail the PL of **TTM-PEG3** under aqueous conditions, PL spectra of **TTM-PEG3** in different ratios of the water/THF (v/v%) mixture were measured (Fig. S15, ESI†).[45] The PL intensity in the 10% water/THF mixture decreased compared to that in pure THF, while the PL intensities in the range from 10% to 90% were almost constant (Fig. S15, ESI†). This suggests that **TTM-PEG3** forms an aggregate when water exists, resulting in concentration quenching of PL. All the radicals showed red to NIR emission in toluene, and **TTM-PEG3** also showed NIR emission in water.

Solvent effect

The solvatofluorochromism was investigated to understand the details of the emission properties of radicals. The PL spectra of radical precursors were measured in toluene. HTTM-OMe3 (precursor) showed a red-shifted PL (367 and 380 nm) derived from the locally excited π^*–π transition of the carbazole unit, compared to HTTM-OMe1 (356 and 373 nm), while their UV-vis absorption peak was almost identical (Fig. S16, ESI†). HTTM-OMe3 is assumed to have a higher HOMO energy level and a smaller HOMO–LUMO gap than HTTM-OMe1 due to the more electron donative methoxy groups. On the other hand, the PL peak of **TTM-OMe3** (radical) (691 nm) was at a shorter wavelength than that of **TTM-OMe1** (729 nm). According to the Lippert–Mataga plots (Fig. S17 and Table S1, ESI†), **TTM-OMe1** was shown to be more sensitive to solvent polarity than **TTM-OMe3**.[46,47] In cyclohexane, **TTM-OMe1** showed a shorter PL wavelength than **TTM-OMe3**, as expected from the bandgap. **TTM-OMe3** has a smaller bandgap and longer PL wavelength in cyclohexane compared to **TTM-OMe1**, but **TTM-OMe1** has a

larger solvent polarity effect that reverses the order in toluene. Similar to the comparison of TTM-OMe radicals, **TTM-PEG3** has a smaller sensitivity to solvent polarity than **TTM-PEG1** (Fig. S17, ESI†). However, the solvent dependence of the Stokes shift of **TTM-PEG3** is rather weak, in highly polar solvents (water and ethanol) and 1,2-dimethoxyethane, which has structural similarity to the PEG chain, and the shift is almost the same around 3000 cm^{-1}. This suggests that the dielectric environment around the **TTM-PEG3** luminophore is constant. Moreover, the actual PL peak of **TTM-PEG3** (777 nm) in water was much shorter than that in water extrapolated from the plot of **TTM-OMe3** (around 929 nm). These results indicate that the **TTM-PEG3** radicals are in a hydrophobic environment (probably aggregates in polar solvents). Thus, the formation of aggregates in water maintains the hydrophobic nature and is assumed to suppress the red-shift of PL, which results in the suppression of the quenching of the PL of **TTM-PEG3** due to the energy gap law.

Photostability

The photostability of new radicals was investigated by monitoring the PL intensity during continuous irradiation with a 355 nm pulsed laser in toluene (Fig. 4). For the investigations, the absorbance of all radicals was controlled to be 0.5 at 355 nm, and the solutions were stirred during the measurement without degassing using a home-made apparatus.[48] The half-lifetimes ($t_{1/2}$) of radicals were determined to be 3.6×10^4 s (**TTM-OMe1**), 7.0×10^4 s (**TTM-OMe3**), 2.8×10^4 s (**TTM-PEG1**), respectively. These $t_{1/2}$ values were slightly longer than that of **TTM-PhCz** (1.6×10^4 s), and drastically improved compared with that of **TTM** (3.3×10^1 s) measured under the same conditions. **TTM-PEG3** showed an increase in PL intensity. This is assumed to be because the original PL intensity of **TTM-PEG3** is weak and degraded compounds show a stronger luminescence. A distinct difference due to the laser irradiation is seen in the time-dependent PL spectra (Fig. S20, ESI†). The PL peak of **TTM-PEG3** after long-term laser irradiation of 3590 seconds was blue-shifted by 18 nm from that after short-term laser irradiation of 20 seconds, namely 732 nm to 714 nm, attributed to a degraded compound, while other radicals show no or quite less blue-shift after long-term irradiation. The degraded compound of **TTM-PEG3** also does not have strong luminescence intensity but it seems to be stronger than that of **TTM-PEG3**. As a result, some increase in the PL intensity was observed for **TTM-PEG3**. New radicals exhibited good photostability under atmospheric conditions.

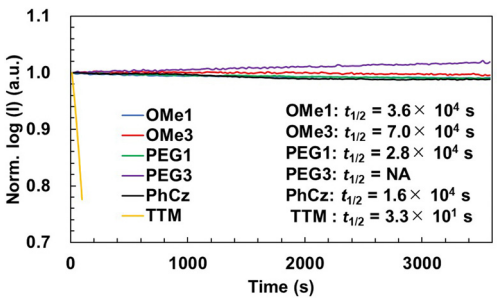

Fig. 4 Photostability of **TTM** radical derivatives measured at an absorbance of 0.5[−] at 355 nm in toluene. $t_{1/2}$ was determined by fitting the results with the equation $I(t) = I_0(1/2)^{\wedge}(t/t_{1/2})$, $I(t)$ is the intensity at a specific time, I_0 is the initial intensity, and t is the time. The plots were shown using the values of moving averages of 10 values over 200 seconds.

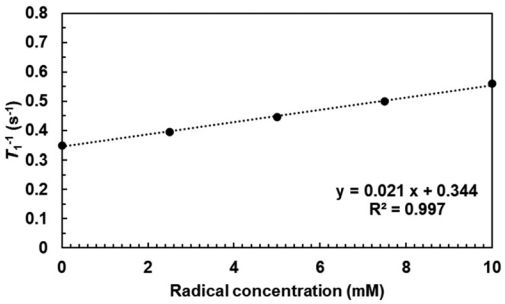

Fig. 5 Plot of T_1 relaxation rates of H_2O protons *versus* the concentration of **TTM-PEG3** in water.

Longitudinal relaxivity

Water-proton longitudinal relaxivity (r_1) of **TTM-PEG3** in an aqueous solution was determined to investigate the potential of **TTM-PEG3** for application as an MRI contrast agent. The longitudinal relaxation time (T_1) of solvent water was measured using a 1 T NMR magnet at different concentrations (Fig. 5). The T_1 relaxation time was shortened by the PRE effect due to the **TTM-PEG3** radicals.[19–22] This result indicates the potential of **TTM-PEG3** for application as an MRI contrast agent. The compatibility of the MRI contrast agent was estimated as the relaxivity value r_1, which was calculated to be 0.02 mM^{-1} s^{-1} using eqn (1).

$$T_1^{-1} = T_0^{-1} + r_1 C \quad (1)$$

T_0 and C denote the T_1 relaxation time without the contrast agent and concentration of the contrast agent, respectively.[20] This r_1 value was smaller than those of the clinically used Gd complex (Gd-DTPA; 3.48 mM^{-1} s^{-1}) and the organic radical TEMPO derivative (2-HEG; 0.41 mM^{-1} s^{-1}) (Fig. S21, ESI†).[21,49] In comparison with Gd, the spin quantum number of organic

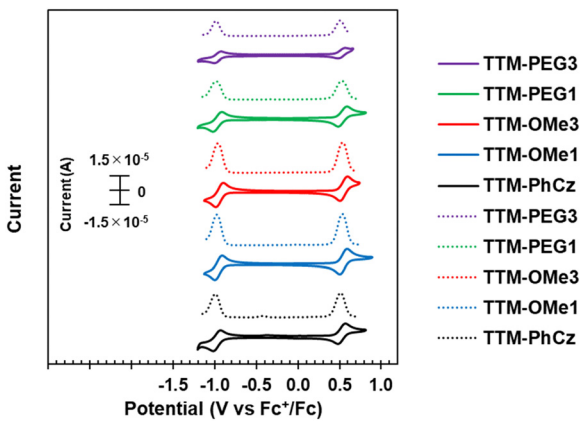

Fig. 6 (Solid line) Cyclic voltammogram (CV) and (dotted line) differential pulse voltammogram (DPV) of **TTM-Cz** derivatives in CH_2Cl_2.

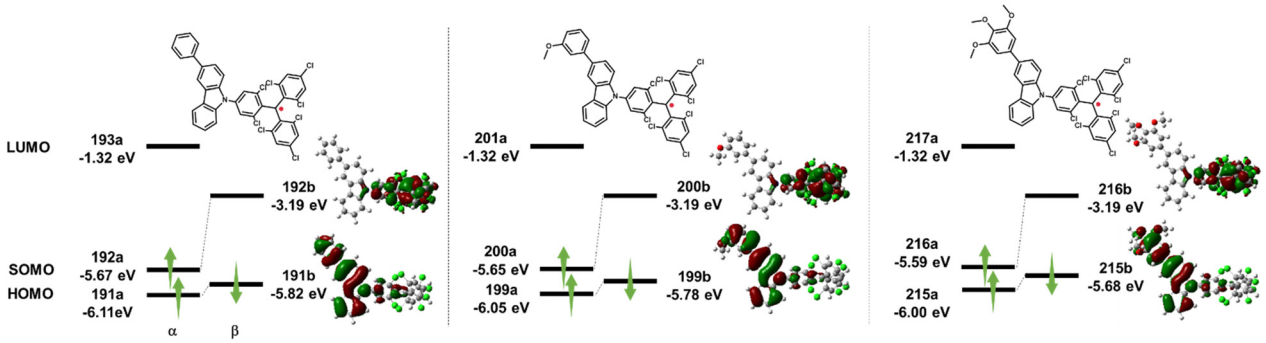

Fig. 7 DFT calculation of HOMO and SOMO energy levels and distributions of molecular orbitals of **TTM-Cz** derivatives at the UPBE0/6-31G(d,p) level of theory.

radicals is small (7/2 *vs.* 1/2). In comparison with organic radicals, the spin quantum number is the same, but the r_1 value of **TTM-PEG3** was 1 order of magnitude smaller than that of 2-HEG. This may originate from the hydrophobicity of the **TTM** unit and aggregate formation, *i.e.*, the relatively small magnetic interactions between **TTM-PEG3** and water molecules. Although r_1 of **TTM-PEG3** is lower than that of conventional radical contrast agents, **TTM-PEG3** is the first **TTM** derivative to show potential for application as an MRI contrast agent.

Electrochemical properties

The electrochemical behavior of new radicals was investigated by cyclic voltammetry (CV) and differential pulse voltammetry (DPV) (Fig. 6). The CV of **TTM-PhCz** was also measured for comparison. All radicals exhibited two similar reversible redox couples at half-wave potentials of −0.96 V/0.53 V *vs.* Fc^+/Fc (**TTM-OMe1**), −0.96 V/0.53 V (**TTM-OMe3**), −0.97 V/0.54 V (**TTM-PEG1**), and −0.97 V/0.52 V (**TTM-PEG3**). These redox potentials were also similar to that of **TTM-PhCz** (−0.98 V/0.53 V) which has no alkoxy group. The redox couple at low voltage is attributed to the reduction of the **TTM** radical and the redox couple at high voltage is attributed to the oxidation of the **TTM** radical.[28] These potentials were nearly identical values, despite that the oxidation potential of the carbazole donor itself, as determined by the CV of the radical precursor, is affected by the alkoxy substituents (Fig. S22, ESI†). These nearly identical potentials were assumed to be due to the approximately 50° torsion between the carbazole donor and the **TTM** unit resulting in minimum electronic communication. All new radicals showed similar redox properties regardless of their substituents.

Theoretical calculations

Unrestricted density functional theory (DFT) calculations using Gaussian 16 with the UPBE0 functional and 6-31G(d,p) basic sets were performed in a vacuum to understand and compare the electronic structures of **TTM-OMe1**, **TTM-OMe3**, and **TTM-PhCz** (Fig. 7).[50] The three radicals were chosen because the PEG chain has too much freedom for calculations, and the electronic structure was assumed to be similar to that of methoxy-substituted radicals. From calculations, the three radicals were found to exhibit similar orbital distributions. The βLUMO (**TTM-PhCz**: 192b, **TTM-OMe1**: 200b, **TTM-OMe3**: 216b) was localized over the TTM moiety, and the βHOMO (**TTM-PhCz**: 191b, **TTM-OMe1**: 199b, **TTM-OMe3**: 215b) was localized over the carbazole moiety. The βHOMO-βLUMO energies were obtained to give an orbital description of the lowest energy absorption band. The energy gaps between the βHOMO and βLUMO were estimated to be 2.20 eV (**TTM-PhCz**), 2.15 eV (**TTM-OMe1**), and 2.05 eV (**TTM-OMe3**). These results indicate the decrease of βHOMO → βLUMO transition energy with the introduction of the methoxy group and the trend matches the absorption maxima of the radicals (Table 1) and describes that the lowest excited state has a CT character.

Conclusions

Alkoxy-group substituted **TTM-Cz** radicals **TTM**-(OMe1, OMe3, PEG1, PEG3) exhibited red to NIR emission, and **TTM-PEG3** is water soluble and showed NIR emission in water. All new radicals exhibited red to NIR emission derived from the CT excited state of the carbazole donor and TTM acceptor. **TTM-PEG3** showed weak NIR emission in water (777 nm) and a water-proton longitudinal relaxivity (0.02 mM^{-1} s^{-1}). To our knowledge, this is the first report of water-proton longitudinal relaxivity of luminescent radicals. These results show their potential for application in fluorescence and MR dual imaging. The simple molecular design strategy allowed the development of water-soluble and luminescent radicals that exhibit magnetic interactions with solvents and have potential applications in bioimaging.

Author contributions

K. Albrecht, and T. H. contributed to the acquisition of the funds for this project. The overall design of the investigation was done by K. Albrecht with assistance from T. H. Most measurements were performed by K. Anraku, with the assistance of K. M., K. Nakamura, K. Nakao, T. H., H. I., and S. M. Water Relaxation time was measured and analyzed by S. O. Major contributions to the data analysis and curation were undertaken by K. Anraku, and T. H. with smaller contributions

from all others. The original draft of the paper was prepared by K. Anraku, and revised based on comments from K. Albrecht, T. H., and S. O. All authors have given approval to the final version of the manuscript.

Conflicts of interest

There are no conflicts to declare.

Acknowledgements

This work was supported, in part, by JSPS KAKENHI Grant No. JP23H02026 and JP23H03966, the Mitsubishi Foundation, and the Cooperative Research Program of ''Network Joint Research Center for Materials and Devices'', and ''Dynamic Alliance for Open Innovation Bridging Human, Environment and Materials'' from MEXT, Japan. This study was also supported by the AIST Nanocharacterization Facility (ANCF) platform as a program of the ''Nanotechnology Platform'' (Grant Number JPMXP09A21AT0017) of MEXT, Japan. The computation was carried out using the computer resource offered under the category of General Projects by the Research Institute for Information Technology, Kyushu University. K. Albrcht thanks Transdisciplinary Energy Research (Q-PIT) through its ''ModuleResearch'' Program at Kyushu University. This work was supported by the Japan Science and Technology Agency (JST) as part of Adopting Sustainable Partnerships for Innovative Research Ecosystem (ASPIRE), Grant Number JPMJAP2334. K. Anraku, and K. Nakamura want to thank Ms Keiko Ideta for helping with ESR measurements. K. Anraku wants to thank Prof. Hajime Nakanotani and Ms Yuika Tamura for helping with PLQY measurements. KM thanks for the support from JST SPRING, Grant Number JPMJSP2136, and Grant-in-Aid for JSPS Research Fellow Grant No. JP24KJ1764. K. Anraku and KM thank Kyushu University Q-PIT Support Program for Young Researchers and Doctoral Students.

References

1 Q. Peng, A. Obolda, M. Zhang and F. Li, *Angew. Chem., Int. Ed.*, 2015, **54**, 7091.
2 P. Murto, R. Chowdhury, S. Gorgon, E. Guo, W. Zeng, B. Li, Y. Sun, H. Francis, R. H. Friend and H. Bronstein, *Nat. Commun.*, 2023, **14**, 4147.
3 X. Bai, W. Tan, A. Abdurahman, X. Li and F. Li, *Dyes Pigm.*, 2022, **202**, 110260.
4 D. Blasi, N. Gonzalez-Pato, X. R. Rodriguez, I. Diez-Zabala, S. Y. Srinivasan, N. Camarero, O. Esquivias, M. Roldán, J. Guasch, A. Laromaine, P. Gorostiza, J. Veciana and I. Ratera, *Small*, 2023, **19**(32), e2207806.
5 L. Chen, T. Rudolf, R. Blinder, N. Suryadevara, A. Dalmeida, P. J. Welscher, M. Lamla, M. Arnold, U. Herr, F. Jelezko, M. Ruben and A. J. C. Kuehne, *Macromolecules*, 2023, **56**, 2104.
6 Y. Xu, C. Teng, H. Dang, D. Yin and L. Yan, *Talanta*, 2024, **266**, 124948.
7 T. P. Nguyen, A. D. Easley, N. Kang, S. Khan, S. M. Lim, Y. H. Rezenom, S. Wang, D. K. Tran, J. Fan, R. A. Letteri, X. He, L. Su, C. H. Yu, J. L. Lutkenhaus and K. L. Wooley, *Nature*, 2021, **593**, 61.
8 Y. Hattori, S. Kimura, T. Kusamoto, H. Maeda and H. Nishihara, *Chem. Commun.*, 2018, **54**, 615.
9 V. S. Mothika, M. Baumgarten and U. Scher, *ACS Appl. Nano Mater.*, 2019, **2**, 4832.
10 L. Zheng, W. Zhu, Z. Zhou, K. Liu, M. Gao and B. Z. Tang, *Mater. Horiz.*, 2021, **8**, 3082.
11 Z. Zhou, J. Qian, K. Liu, Y. Zhang, M. Gao and B. Z. Tang, *Angew. Chem., Int. Ed.*, 2022, **61**, e2022126.
12 M. Ballester, *Bull. Soc. Chim. Fr.*, 1966, 7.
13 O. Armet, J. Veciana, C. Rovira, J. Riera, J. Castaner, E. Molins, J. Rius, C. Miravitlles, S. Olivella and J. Brichfeus, *J. Phys. Chem.*, 1987, **91**, 5608.
14 G. R. Luckhurst and J. N. Ockwell, *Tetrahedron Lett.*, 1968, **9**, 4123.
15 M. A. Fox, E. Gaillard and C. C. Chen, *J. Am. Chem. Soc.*, 1987, **109**, 7088.
16 V. Gamero, D. Velasco, S. Latorre, F. Lopez-Calahorra, E. Brillas and L. Julia, *Tetrahedron Lett.*, 2006, **47**, 2305.
17 H. Guo, Q. Peng, X. Chen, Q. Gu, S. Dong, E. W. Evans, A. J. Gillett, X. Ai, M. Zhang, D. Credgington, V. Coropceanu, R. H. Friend, J. Brédas and F. Li, *Nat. Mater.*, 2019, **18**, 977.
18 H. Imahori, Y. Kobori and H. Kaji, *Acc. Mater. Res.*, 2021, **2**, 501.
19 C. Yan, D. An, W. Chen, N. Zhang, Y. Qiao, J. Fang, X. Lu, G. Zhou and Y. Liu, *CCS Chem.*, 2022, **4**, 3190.
20 Y. Hattori, T. Kusamoto and H. Nishihara, *Angew. Chem., Int. Ed.*, 2014, **53**, 11845.
21 K. Morishita, S. Murayama, T. Araki, I. Aoki and S. Karasawa, *J. Org. Chem.*, 2016, **81**, 8351.
22 K. Morishita, Y. Okamoto, S. Murayama, K. Usui, E. Ohashi, G. Hirai, I. Aoki and S. Karasawa, *Langmuir*, 2017, **33**(31), 7810.
23 K. Morishita, S. Ueki, Y. Fuchi, S. Murayama, T. Kaneko, N. Narita, S. Kobayashi, G. Hirai, I. Aoki and S. Karasawa, *ACS Appl. Nano Mater.*, 2018, **1**, 6967.
24 R. Shiraishi, T. Kaneko, K. Usui, T. Naganuma, N. Iizuka, K. Morishita, S. Kobayashi, Y. Fuchi, Y. Matsuoka, G. Hirai, K. Yamada and S. Karasawa, *ACS Omega*, 2019, **4**, 20715.
25 S. Okada, S. Mizukami and K. Kikuchi, *ChemBioChem*, 2010, **11**, 785.
26 J. O. Lagerstedt, J. Petrlova, S. Hilt, A. Marek, Y. Chung, R. Sriram, M. S. Budamagunta, J. F. Desreuxd, D. Thonond, T. Jue, A. I. Smirnov and J. C. Voss, *Contrast Media Mol. Imaging*, 2013, **8**, 252.
27 E. G. Ankel, C. Lai, L. E. Hopwood and Z. Zivkovic, *Life Sci.*, 1987, **40**(5), 495.
28 O. Armet, J. Veciana, C. Rovira, J. Riera, J. Castaner, E. Molins, J. Rius, C. Miravitlles, S. Olivella and J. Brichfeus, *J. Phys. Chem.*, 1987, **91**(22), 5608.
29 D. Velasco, S. Castellanos, M. López, F. López-Calahorra, E. Brillas and L. Juliá, *J. Org. Chem.*, 2007, **72**(20), 7523.

30 K. Matsuda, R. Xiaotian, K. Nakamura, M. Furukori, T. Hosokai, K. Anraku, K. Nakao and K. Albrecht, *Chem. Commun.*, 2022, **58**, 13443.
31 K. Nakamura, K. Matsuda, R. Xiaotian, M. Furukori, S. Miyata, T. Hosokai, K. Anraku, K. Nakao and K. Albrecht, *Faraday Discuss.*, 2024, **250**, 192.
32 R. Xiaotian, W. Ota, T. Sato, M. Furukori, Y. Nakayama, T. Hosokai, E. Hisamura, K. Nakamura, K. Matsuda, K. Nakao, A. P. Monkman and K. Albrecht, *Angew. Chem., Int. Ed.*, 2023, **62**, e202302550.
33 J. A. Mesa, A. Velázquez-Palenzuela, E. Brillas, J. Coll, J. L. Torres and L. Juliá, *J. Org. Chem.*, 2012, **77**(2), 1081.
34 J. A. Mesa, A. Velázquez-Palenzuela, E. Brillas, J. L. Torres and L. Juliá, *Tetrahedron*, 2011, **67**, 3119.
35 A. Carreras, J. A. Mesa, M. Cascante, J. L. Torres and L. Juliá, *New J. Chem.*, 2013, **37**, 2043.
36 A. Boś-Liedke, M. Walawender, A. Woźniak, D. Flak, J. Gapiński, S. Jurga, M. Kucińska, A. Plewiński, M. Murias, M. Elewa, L. Lampp, P. Imming and K. Tadyszak, *Cell Biochem. Biophys.*, 2018, **76**, 19.
37 M. E. Arnold, L. Schoeneburg, M. Lamla and A. J. C. Kuehne, *Molecules*, 2024, **29**, 995.
38 Z. S. Parr, R. B. Rashid, B. D. Paulsen, B. Poggi, E. Tan, M. Freeley, M. Palma, I. Abrahams, J. Rivnay and C. B. Nielsen, *Adv. Electron. Mater.*, 2020, **6**, 2000215.
39 T. Yasuda, T. Shimizu, F. Liu, G. Ungar and T. Kato, *J. Am. Chem. Soc.*, 2011, **133**(34), 13437.
40 B. Cheng, G. Zhu, L. Meng, G. Wu, Q. Chen and S. Ma, *Eur. J. of Med. Chem.*, 2022, **228**, 113930.
41 A. Abdurahman, Q. Peng, O. Ablikim, X. Ai and F. Li, *Mater. Horiz.*, 2019, **6**, 1265.
42 H. Maeda, Y. Ito, Y. Haketa, N. Eifuku, E. Lee, M. Lee, T. Hashishin and K. Kaneko, *Chem. – Eur. J.*, 2009, **15**, 3706.
43 A. Abdurahman, T. J. H. Hele, Q. Gu, J. Zhang, Q. Peng, M. Zhang, R. H. Friend, F. Li and E. W. Evans, *Nat. Mater.*, 2020, **19**, 1224.
44 K. Nakamaru, *Bull. Chem. Soc. Jpn.*, 1982, **55**, 2697.
45 S. S. Liow, H. Zhou, S. Sugiarto, S. Guo, M. L. S. Chalasani, N. K. Verma, J. Xu and X. J. Loh, *Biomacromolecules*, 2017, **18**, 886.
46 N. Mataga, Y. Kaifu and M. Koizumi, *Bull. Chem. Soc. Jpn.*, 1956, **29**, 465.
47 J. P. Cerón-Carrascoa, D. Jacquemina, C. Laurencea, A. Planchata, C. Reichardtc and K. Sraïdi, *J. Phys. Org. Chem.*, 2014, **27**, 512.
48 M. Furukori, Y. Nagamune, Y. Nakayama and T. Hosokai, *J. Mater. Chem. C*, 2023, **11**, 4357.
49 P. Mi, D. Kokuryo, H. Cabral, M. Kumagai, T. Nomoto, I. Aoki, Y. Terada, A. Kishimura, N. Nishiyama and K. Kataoka, *J. Controlled Release*, 2014, **174**, 63.
50 M. J. Frisch, *et al.*, *Gaussian 16, Revision C.01*, Gaussian, Inc., Wallingford CT, 2016.

